CHARACTERISTICS OF EARLY EARTH'S CRITICAL ZONE BASED ON MIDDLE−LATE DEVONIAN PALEOSOL PROPERTIES (VORONEZH HIGH, RUSSIA)

Tatiana Alekseeva[1],*, Pavel Kabanov[2], Andrey Alekseev[1], Pavel Kalinin[1], and Veronika Alekseeva[3]

[1] Institute of Physical, Chemical, and Biological Problems of Soil Science, Russian Academy of Sciences, ul. Institutskaya, 2, Pushchino, 142290, Russia
[2] Geological Survey of Canada, 3303 33rd Street N.W., Calgary, Alberta, Canada T2L 2A7
[3] Faculty of Geography, Moscow State University, Leninskie Gori, Moscow, 119999, Russia

Abstract—Land colonization with vascular plants during the late Silurian−early Devonian and then arborescence during the Pragian−Givetian caused the development of new soil types. These true-rooted soils increased the rate of pedogenesis on a global scale. Since that time, soil has become a key component of the biosphere and has given rise to profound development of the Earth's Critical Zone (CZ). Case studies of Devonian CZs have helped to record the transformation from Precambrian−Lower Paleozoic 'proto-CZs,' which had insufficient proto-soil cover, to modern soils with true-rooted pedosphere. Devonian (Givetian−Frasnian) paleosols from the Voronezh region of Russia are combined into pedocomplexes which occupied the top, slope, and bottom positions of a pronounced paleo-relief. Paleosols were developed from terrigenous argillites and volcanigenic-sedimentary deposits. Each pedocomplex consisted of four or more paleosols with different degrees of development and profile preservation. Paleosols exhibited several common characteristics including production and translocation of clay, ferruginization and the presence of siderite nodules, enhanced MnO/Al_2O_3 and $(Fe_2O_3+MnO)/Al_2O_3$ values, and *in situ* roots and root-system traces. The latter are siderite/goethite substituted. Stable isotope analysis of siderite shows $\delta^{13}C$ values of between −6.1 and −13.7‰ indicating that CO_2 had originated from C_3 plants. The main mineral component of clay fractions in automorphic paleosols (top and slope of the paleorelief) is kaolinite. The important feature of these paleosols is the red-stained hematite-rich layer in their bases. These horizons developed at different depths and with different thicknesses, and marked the paleo-groundwater tables of each sub-CZ. Evidence of the imprints of vegetation is seen in the abundant *in situ* roots, plant fragments, and spores of rhyniophytes, lycopsids, progymnosperms, cladoxylalean ferns, and phytoleims of algae-like vascular plants. The near-equatorial location and the overall characteristics of paleosols studied suggest that the aforementioned horizons were formed in a tropically warm and humid climate. The paleo-ecological environments which accompanied pedogenesis were probably controlled by tectonic activity and volcanism.

Key Words—Central Devonian Field, Clay Mineralogy, Devonian Paleosols, Devonian Roots, Mineral Weathering, Paleo-Critical Zone, Voronezh Anteclise.

INTRODUCTION

In response to the growing demand for conceptual bundling of land-surface studies (Lin, 2010; Giardino and Houser, 2015), the Earth's Critical Zone has been defined as a range of terrestrial environments extending from vegetation crown down to deep subsoil aquifers. Although the Earth's terrestrial vegetation first appeared in the early−middle Ordovician, those plants were small, non-vascular, and thalloid. The abundance of vascular plants was extended during the late Silurian−early Devonian. These plants were small, non-rooted, or shallow rooted, however, with limited distribution restricted to moist lowland territories which had little effect on their habitats. Plant-substrate interactions intensified significantly with the appearance of deep-rooted arborescent vegetation in the middle−late Devonian (Algeo and Scheckler, 1998). The expansion of rooted soils that were able to stabilize land surfaces has been recorded through the Devonian (Hillier *et al.*, 2008; Davies and Gibling, 2010). In the Carboniferous, thick-rooted paleosols expanded to fairly dry landscapes (Kabanov *et al.*, 2010; Tabor and Myers, 2015). Most of the major soil types first appeared during the Devonian−Carboniferous (Retallack, 2001). Studies of pre-Quaternary (especially Paleozoic) palaeosols in the context of CZ science are in their infancy (Nordt *et al.*, 2012; Nordt and Driese, 2014). Case studies of Devonian CZs are important, therefore, as they record transformation from Precambrian−Lower Paleozoic 'proto-CZs' with insufficient protosoil cover to those

* E-mail address of corresponding author:
alekseeva@issp.serpukhov.su

with a true-rooted pedosphere. The true-rooted pedo-sphere stabilized the ground, allowing more time for substrate disintegration and weathering (including chemical weathering by means of the production of root exudates and generation of excess soil pCO$_2$ *via* oxidation of organic matter) (Algeo and Scheckler, 1998; Amundson *et al*., 2007; Chorover *et al*., 2007; Zavarzin, 2008; Davies and Gibling, 2010; Giardino and Houser, 2015).

Records of Devonian paleosols from Russia are rare (*e.g*. Shumilov and Mingalev, 2009; Shumilov, 2010, 2013). The present study describes middle−late Devonian pedocomplexes from the eastern flank of the Voronezh crystalline massif by adding more detailed information to existing preliminary notes on sedimentary disconformities, fossil plant, and spore associations from this thin sedimentary succession of Givetian−Frasnian age (Rodionova *et al*., 1995; Raskatova, 1990, 2004).

GEOLOGICAL SETTING

The late Givetian−Lower Frasnian paleosols are found in the Shkurlat granite quarry near the town of Pavlovsk (50º23′N, 40º13′E) (WGS84) (Figure 1a,b). Geologically, the area occurs on the eastern slope of the Voronezh Massif, one of major highs in the Precambrian crystalline basement of the East European Craton separating the Moscow and Donets basins (Nikishin *et al*., 1996). Throughout most of the Phanerozoic, the Voronezh Massif remained uplifted as indicated by siliciclastics in surrounding basins (*e.g*. Kabanov *et al*., 2014; Alekseev *et al*., 2015). Paleozoic lithostratigraphic units in the central part of the Massif tend to pinch out and bear shallow-water and weathering features indicating protracted periods of subaerial exposure. Based on paleobiogeographic reconstructions, the Voronezh Massif, including its flanks, remained largely uplifted during the Devonian and was connected to the Old Red Sandstone paleo-continent to the west (Lebedev *et al*., 2010).

The Devonian strata are 7−20 m thick in the Shkurlat Quarry, filling lows in the deeply weathered (lateritized) top of the Proterozoic granite. The base of the Devonian section is composed of marine shales, siltstones, and very fine-grained sandstones bearing horizons of carbonate nodules. This basal unit, correlated to the Starooskolian Regional Substage of the Givetian Stage, contains sporadic marine fauna of brachiopods, rugose corals, gorefish fragments, small bioherms, and a horizon of large (5−7 cm) oncoids. The Starooskolian marine deposits contain 40−16% of clay, mostly kaolinite. Siderite is present in the rock matrix in amounts of 4−5%. Carbonate concretions and stromatolitic nodules are also dominated by siderite. The upper part of the marine shales has been eroded intensively.

The upper 3.0−6.0 m of the Devonian section is non-marine and is correlated with the Starooskolian

(Givetian) and Yastrebovka (early Frasnian) Formations (Raskatova, 1990, 2004); it consists of the claystone unit (1.5−2.5 m) and the upper volcaniclastic sandstone unit (Figure 2). The Devonian is overlapped by the Cretaceous, Pleistocene, and Holocene sediments with a total thickness of 35 m.

The paleosols studied belong to the Starooskolian/Yastrebovka Formations. Samples were collected during the summer field seasons in the period 2010−2015 from different locations above a channel-like lenticular body. The paleo-channel is 500 m across from its center to the left margin and reached a thickness of 15 m in the center. It is filled with several stacked units of Yastrebovka Formation volcaniclastic sediments containing abundant plant debris including stem fragments and stumps. Plant fragments are coalified and pyritized, but retain significant tissue structure. The cross sections of the channel and sampling-site locations are depicted in Figure 2.

METHODS

The granulometric composition of carbonate-free samples, organic carbon (OC), and carbonate contents were measured by standard soil-science procedures (van Reeuwijk, 2002). Fourier-transform infrared (FTIR) spectra were recorded using a ThermoFisher Nicolet 6700 spectrometer and employing the KBr pellet technique (1 mg of sample and 199 mg of KBr). Magnetic susceptibility (MS) was measured using a KLY-2 Kappabridge device (Advanced Geoscience Instruments Co., Brno, Czech Republic). Three measurements were taken for each sample. Each was weighed with a precision of 0.01 g, using normalized data on mass-specific MS (χ) expressed as $\times 10^{-8}$ m^3 kg^{-1}.

Bulk and clay mineralogy

The bulk and clay mineralogy were estimated from X-ray diffraction (XRD) patterns taken using a Bruker D2 Phaser instrument (Bruker Corporation, Billerica, Massachusetts, USA), with CuKα radiation, at 0.1º2θ scan step and a count time of 10 s per step. The whole-rock and pedo-feature (nodules, root replacements, *etc*.) mineralogy were studied using the randomly oriented specimens prepared with ethyl alcohol. The clay fraction (<2 μm) was separated by sedimentation from the insoluble residue after carbonate removal by the buffered acetic acid solution (van Reeuwijk, 2002). Parallel oriented specimens of clay fractions were prepared by sedimentation from their water suspensions on a glass slide (15 mm × 15 mm). The following set of treatments was applied in the identification of clay minerals: (1) Mg^{2+} saturation at room temperature; (2) Mg^{2+} and ethylene-glycol saturation for 24 h at room temperature; (3) Mg^{2+} saturation and heating at 350ºC for 2 h; (4) Mg^{2+} saturation and heating at 550ºC for 2 h; (5) K$^+$ saturation at room temperature; (6) K$^+$
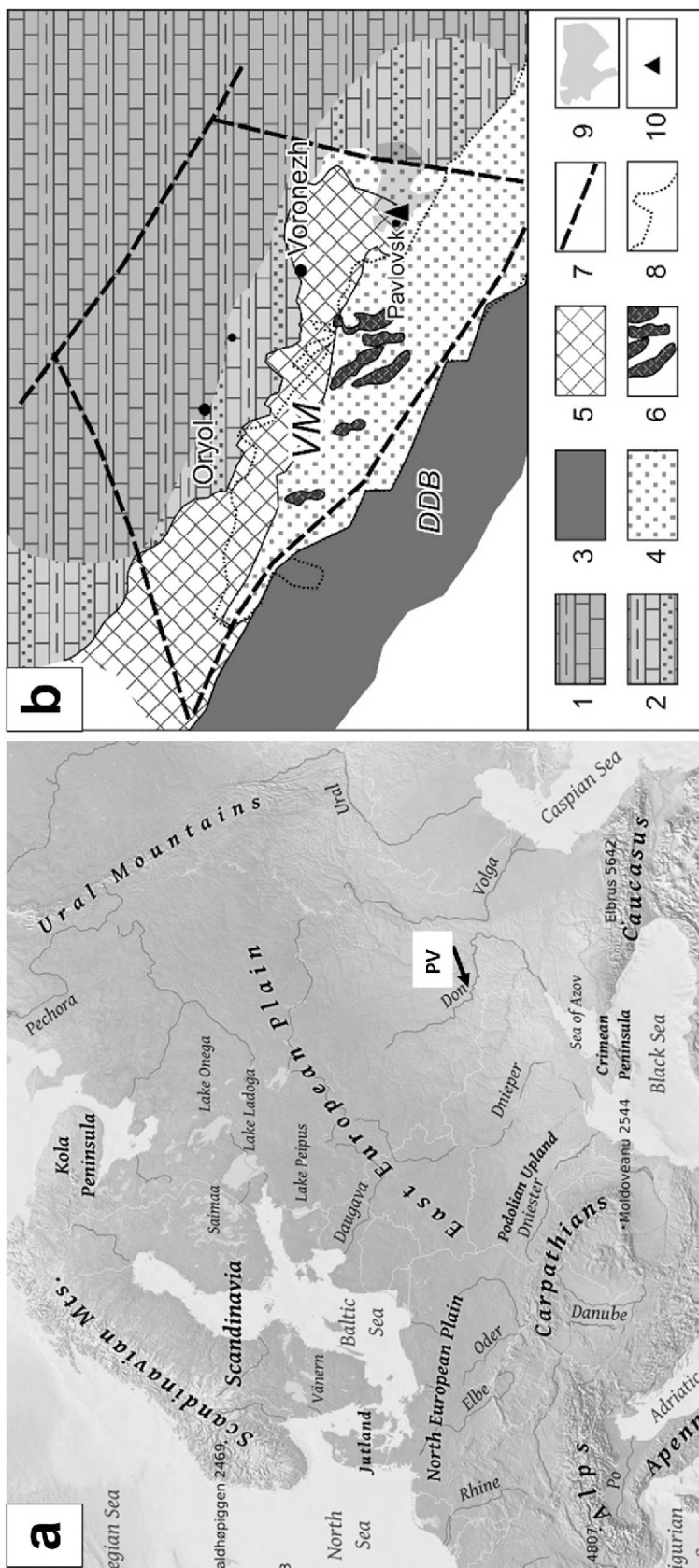
Figure 1. Location of the study area: (a) Pavlovsk (PV) on a modern map of Europe; (b) Pavlovsk on the late Frasnian paleogeographic map of the Voronezh Massif (VM) and lithologo-paleogeographic elements of Yastrebovka Formation (modified from Shevyrev et al., 2004). Legend: (1) limestones with minor siliciclastics, shallow shelf zone; (2) alternating limestones, sandstones, and shales, shallow subtidal to shoreface to onshore zone; (3) undivided deposits of the Dnieper-Donetz rifted basin (DDB); (4) fluvial plain deposits; (5) late Frasnian denudation zone; (6) trap basalts; (7) major normal faults as boundaries of the Voronezh Massif; (8) late Givetian denudation area; (9) volcanic rocks of the Yastrebovka formation; (10) the studied section.
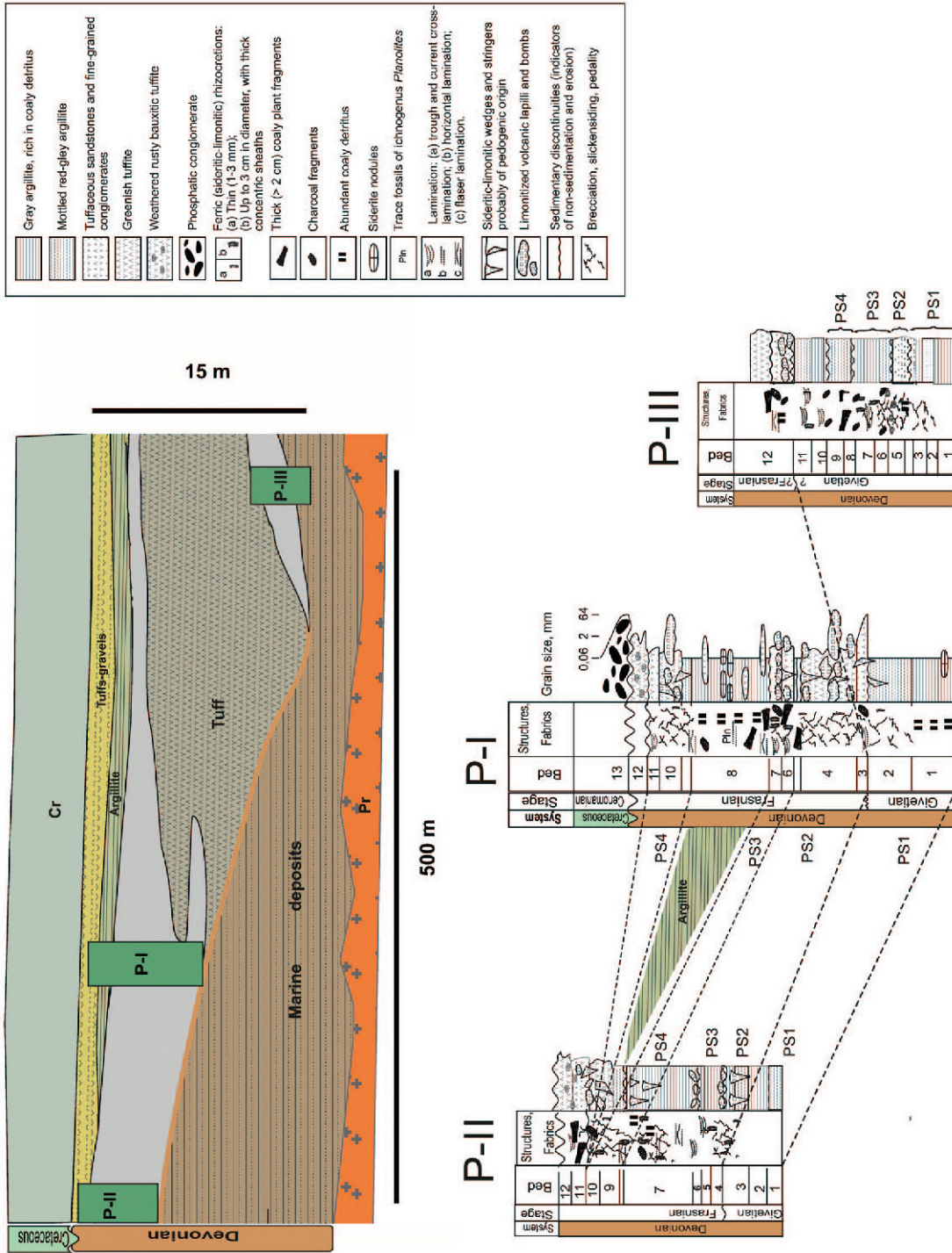
Figure 2. Schematic image of the southeast wall of the Pavlovsk quarry where the paleosols were discovered: geology, lithology, and pedocomplex locations. Abbreviated notations: Pr – Proterozoic platform; Cr – Cretaceous deposits; P-I, P-II, and P-III – pedocomplexes I, II, and III, respectively. PS1–PS4 – paleosols of each pedocomplex with independent internal numbering. Figure not drawn to scale in either the horizontal or vertical direction.

and ethylene-glycol saturation for 24 h at room temperature; (7) Li$^+$ saturation, heating at 250ºC for 24 h, and ethylene-glycol solvation for 24 h.

Elemental chemical compositions

Elemental concentrations were determined using a desktop X-ray fluorescence crystal diffraction scanning spectrometer from SPECTROSCAN MAKC-GV (St. Petersburg, Russia). The quantitative analysis methods were based on the 24 standard rock and soil samples. To quantify the weathering intensity, different elemental ratios were applied (Retallack, 2001; Sheldon and Tabor, 2009).

Carbon isotopic composition of carbonate (siderite)

The $^{13}C/^{12}C$ carbon isotope ratios of carbonate were measured using an isotope ratio mass spectrometer (IRMS) (GV Isoprime, UK). The nodular carbonate (siderite) samples were analyzed. CO_2 from siderite was extracted with 100% phosphoric acid at 50ºC for periods ranging from 1 to 10 days. The measurements were performed using an autosampler and heated sample tray for reaction vials connected to the IRMS using continuous-flow mode. Isotopic compositions were measured against internal standards and are reported in the standard δ notation as per mil (‰) deviation from V-PDB (Vienna-Pee Dee Belemnite). The values obtained after different contact time with phosphoric acid show some difference in terms of δ^{13}C depletion with time. For the discussion below, the mean values obtained after the 4th and 10th days of contact were used. The standard deviation of replicate measurements of standards was 0.1‰.

Micromorphological study

The micromorphology of undisturbed whole-rock samples and of morphologically observable pedo-features (nodules, root replacements) was examined using scanning electron microscopy/energy-dispersive X-ray spectrometry (SEM/EDS) (TESCAN Vega 3) (TESCAN, Brno, Czech Republic). The SEM was also used to describe the micromorphology of the quartz and other detrital mineral grain surfaces in the size range 0.25−0.50 mm after treatment with 10% HCl (Alekseeva, 2005).

RESULTS

Host rocks

Most of the paleosol-hosting section belongs to the Yastrebovka Formation. Mineralogical and petrographic observations revealed volcaniclastic and tuffaceous facies. The tuffaceous facies contains pebble- to cobble-sized, nodule-like features decomposed largely into soft limonitic mass and interpreted as lapilli (2−60 mm) and bombs (up to 25 cm). The presence of these features indicates a proximal eruption source

probably of kimberlite type (Shevyrev *et al.*, 2004; Zolotareva, 2009). Nine samples of tuffaceous rocks were collected from this formation across the quarry. The most abundant minerals in the samples studied are quartz, kaolinite, and feldspars. The amounts present of the main chemical elements studied varied significantly: 41.09−72.46% SiO_2; 10.43−26.87% Al_2O_3; 3.14−27.59% Fe_2O_3; 1.49−14.86% TiO_2; 0.41−4.44% MgO; 0.10−2.42% K_2O; 0.14−1.28% CaO; 0.45−2.88% Na_2O; 0.08−0.39 P_2O_5; 0.07−0.29% S; 0.01−0.09% MnO; 0.01−0.12% V; 0.01−0.13% Cr, and the sum of the above elements ranged from 96 to 99%.

The non-marine Starooskolian and Yastrebovka deposits contain up to four stacked paleosols. Depending on their location in the paleo-relief, they are attributed to three pedocomplexes abbreviated as P-I (channel-bank slope), P-II (bank top), and P-III (channel bottom) (Figure 2).
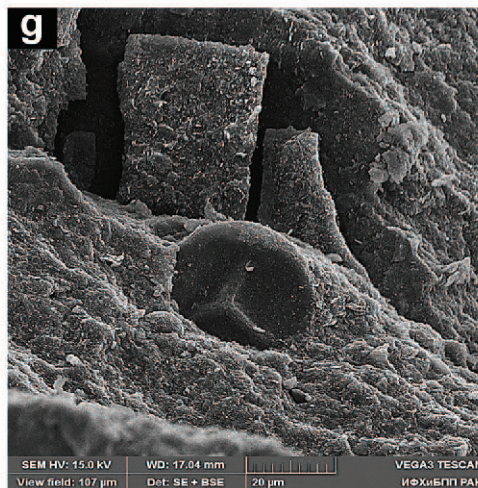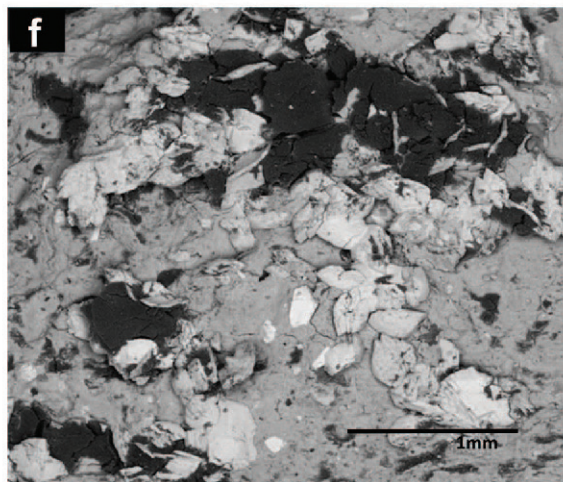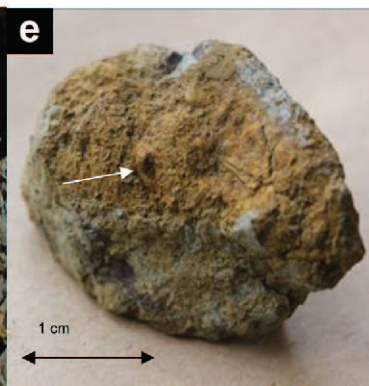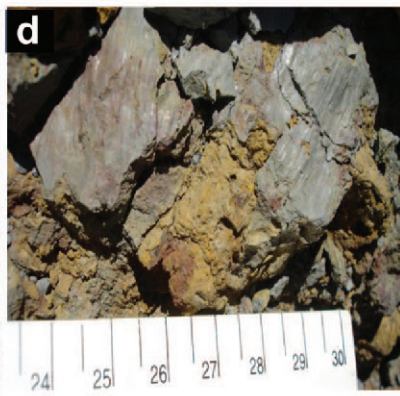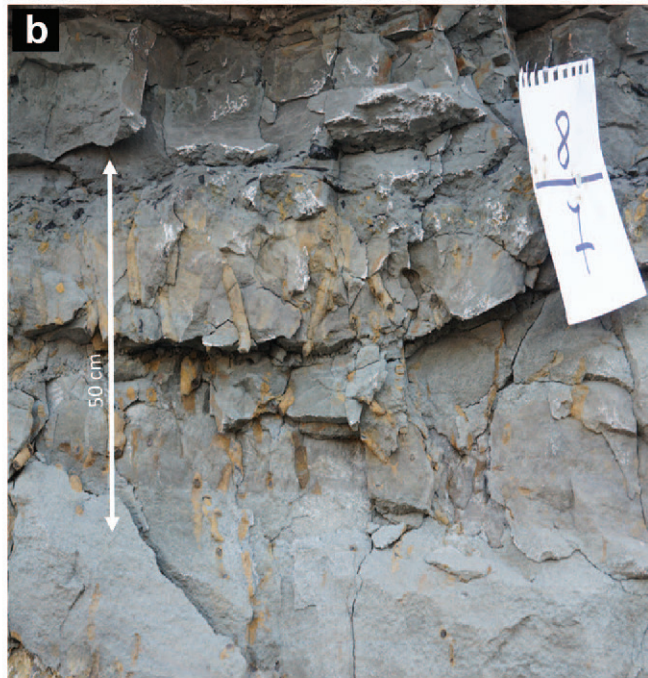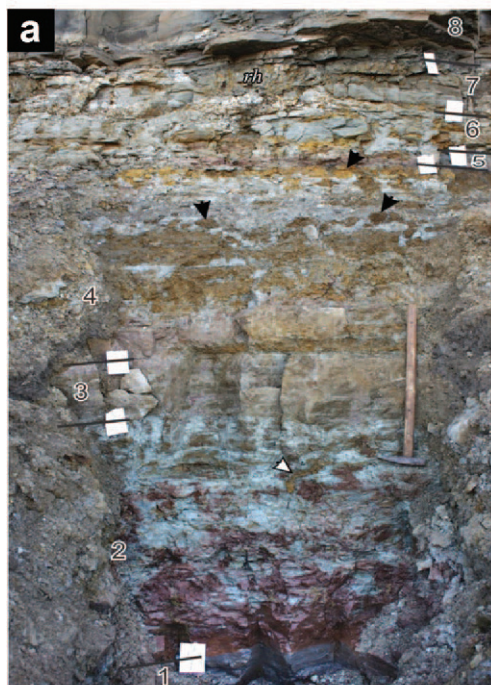
Pedocomplex I

Description. Pedocomplex I (P-I in Figure 2), developed on the slope of the paleo-channel, consists of four paleosols. The pedocomplex is 6 m thick in total. The lowermost paleosol (PS1) in the formation base developed on Starooskolian shales; other paleosols developed from Yastrebovka volcanigenic-sedimentary deposits. The paleosol profiles have different thicknesses (Figure 3a). The composite profile of PS1 and PS2 is 1.5 m. The thinnest paleosol, PS3, is 60 cm thick and is covered with a layer of coalified plant litter and stands out because of the presence of spectacular pipe-like limonitic-sideritic rhizocretions which are 1 cm in diameter and up to 15 cm in traced length (Figure 3b,c). In better preserved rhizocretions, root parenchyma and bark have been replaced by siderite, and the central canal remains either empty or is filled with a siderite, goethite, or pyrite. PS3 is overlain by thick (up to 2 m), hard argillite (bed 8 in Figure 3a). This layer has no pedogenic features and contains *Planolites* bioturbation features and rare marine fauna associated with the estuarian sediments deposited during the short catastrophic flooding of the territory. The PS4 located above the argillite layer (beds 9−11 in Figure 2) is automorphic (formed *in situ*) and oxidized intensively.

Paleosols of P-I exhibit accumulations of organic matter and carbonate and redistribution of clay and chemical elements (Figure 4). The lowest pedogenic horizons of each individual paleosol profile are red stained to various degrees (Figure 3a). Organic matter is present as the coalified organic macro/micro particles, spores, *in situ* roots, and root canals. PS1 is clayey; the others are sandy (Figure 4).

Paleosol-associated carbonates

The specific feature of paleosols is the presence of abundant siderite nodules (color 2.5Y 4/4). Nodules are rounded or irregular with a diameter of 1 cm up to
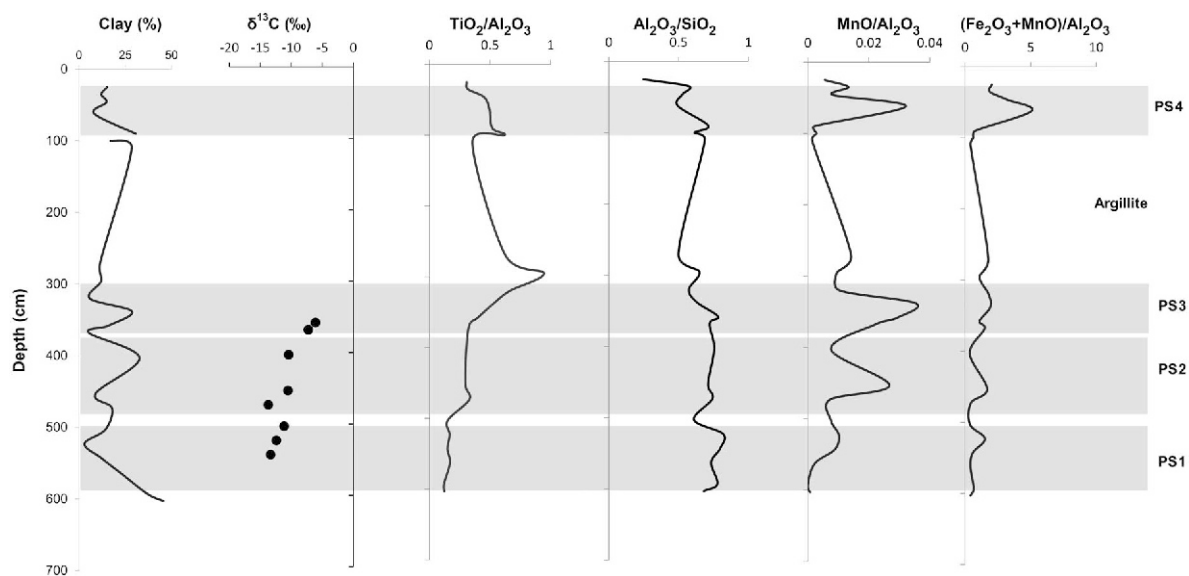
Figure 4. Selected analytical data from pedocomplex I.

10−15 cm (Figure 3d,e). Aside from the siderite they contain varying amounts of goethite, quartz, and kaolinite. Many of the nodules have petrographic features which reflect preservation of roots (Figure 3e). In some cases the density and interlacing of roots resulted in their intergrowth with development of larger-scale pedofeatures, which are frequently surrounded by better preserved root casts from later stages. The outer surfaces of nodules tend to be covered by argillans (clayey cutans) formed by clay illuviation processes (Figure 3d). A similar mode of root preservation within calcitic carbonate nodules has been described (Cox *et al.*, 2001) for the middle−late Devonian paleosols of the Catskill Formation, New York.

The $\delta^{13}C$ of siderite nodules from PS1, PS2, and PS3 ranges between −6.1 and −13.7‰ with an average of −9.8‰, typical of a pedogenic origin and a C_3 plant source of CO_2, and is within the range of biogenic carbonate (Zamanian *et al.*, 2016). In the latter case CO_2/HCO_3^- were apparently produced by anaerobic microbial oxidation of organic matter with subsequent siderite formation under occasionally (or seasonally) water-logged environments (Wilkinson *et al.*, 2000; Weibel *et al*., 2016). The data presented here, which demonstrate depletion of $\delta^{13}C$ with depth, may indicate an increase in the microbial pull of CO_2 in the lower part of P-I. This may also reflect a microbial (bacteria and fermenters) variety, which produced CO_2/HCO_3^- for siderite precipitation (Weibel *et al.*, 2016).

These values are in the range reported by Driese and Mora (1993) for pedogenic Mg/Mn/Fe carbonates in the Catskill Formation, by Cox *et al.* (2001) for pedogenic calcite at the same location, by Quast *et al.* (2006) for Lower Devonian−Lower Carboniferous pedogenic Ca-Mg carbonates from the UK and western Europe, and by Brasier *et al.* (2014) for pedogenic calcite from Old Red Stone of south Wales (UK).

Mineralogy

The whole-rock samples of all paleosols in P-I are dominated by kaolinite (Figure 5a,b). In addition, some layers contain different proportions of quartz and Fe-bearing minerals: goethite, hematite, siderite, and ilmenite. Kaolinite from different paleosols varies in terms of the degree of ordering. The largest degree of kaolinite ordering occurs in Starooskolian PS1: its XRD patterns have the narrowest peaks at 4.36 Å ($1\bar{1}0$) and 4.18 Å ($11\bar{1}$). The FTIR spectra of PS1 exhibit three vibration bands of OH-stretching groups of the octahedral sheet: two well developed at 3620 and 3700 cm^{-1}, and a small peak at 3655 cm^{-1} (Figure 5c). Kaolinites from the Yastrebovka Formation PS2 and PS3 have one broad XRD peak at 4.48 Å (020). The FTIR spectra of these kaolinites indicate the presence of only one

Figure 3 (*facing page*). Pedocomplex I. (a) Hematitic red layer at the base. Abbreviations: rh − roots; numbers (1−8) indicate the beds described; (b) paleosol 3 (beds 6−7 in part a) with rooting systems and coalified organic matter at the top; (c) rooting systems of PS3; (d) oriented clay cutans on the surfaces of siderite concretions; (e) siderite concretion with a mineralized root (arrow); (f) autigeneous goethite crystals (white) in association with organic debris (black) from bed 7; (g) *in situ* spore of *Tanaitis furcihasta* from the litter layer of PS3 (bed 7).
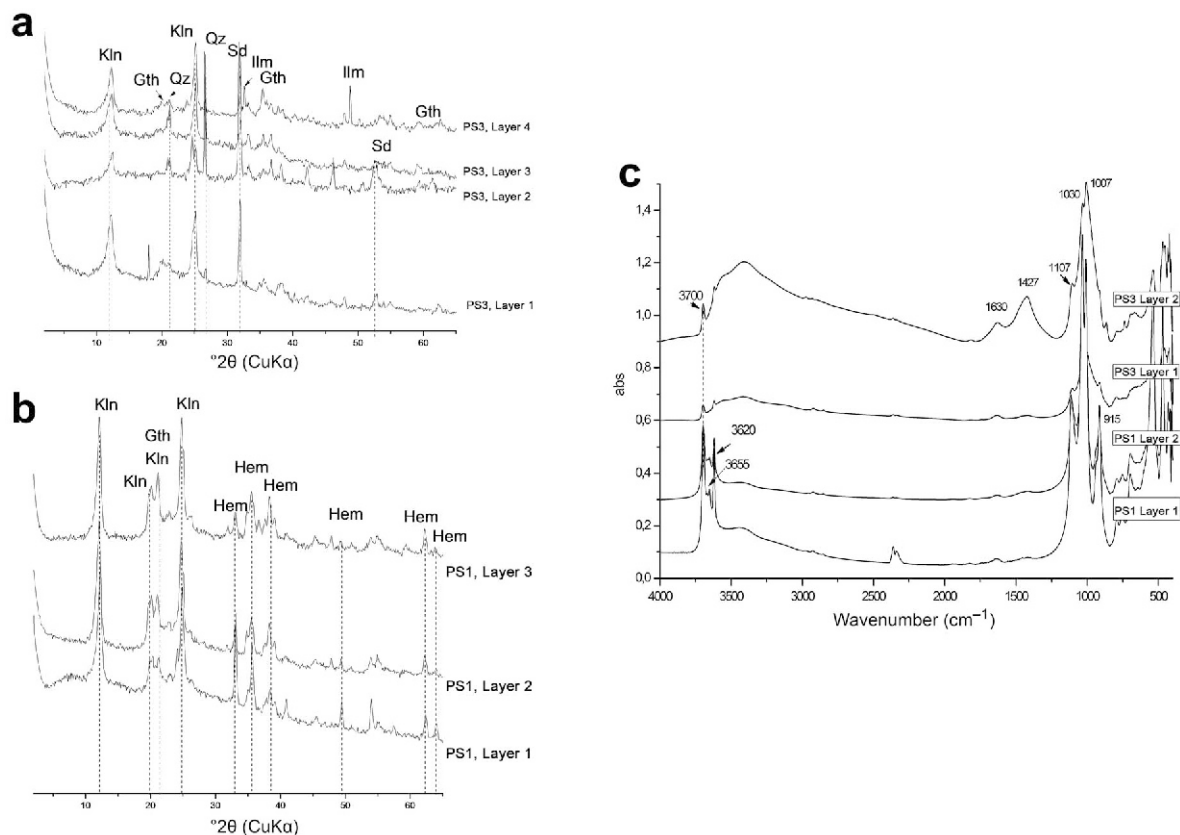
Figure 5. Whole-rock mineralogy of paleosols from pedocomplex I. (a) XRD patterns of selected layers from paleosol 3; (b) XRD patterns of selected layers from paleosol 1; (c) FTIR spectra of selected samples. Kln − kaolinite; Gth − goethite, Hem − hematite; Sd − siderite; Ilm − ilmenite; Qz − quartz.

intensive peak at 3700 cm^{-1}. The peak at ~3400 cm^{-1}, present in all spectra, belongs to OH-stretching of water in kaolinite, hydrogoethite, or other amorphous hydrated oxides; it has different intensities with a maximum for PS3 bed 2 where the supplementary peak at 1630 cm^{-1}, belonging to OH-deformation of water, appeared. The intense band at 1427 cm^{-1} in this spectrum reflects CO$_3$-stretching of siderite. The degree of kaolinite ordering was shown by Levikh (1988) and Kornilovich (1994) to depend on the precursor mineral(s) and weathering (such as leaching) conditions. Kaolinites derived from the pre-Devonian granite weathering crust appear to have more ordered structures than those developed from volcanigenic material of the Yastrebovka Formation.

All paleosols of P-I have similar clay mineralogy: some horizons are monomineralic, *i.e.* consisting of kaolinite, the others also contain goethite (Figure 6a,b). The present SEM study of the undisturbed sample from the top layer of PS3 (bed 7) shows μm-sized goethite crystals closely associated with organic particles (Figure 3f). The mineral association of paleosols indicates strong soil leaching in humid tropical climates, a long duration of the pedogenesis as well as good drainage (Tabor and Myers, 2015). The *in situ* origin of kaolinite in PS2, PS3, and PS4 is supported by the SEM study of

quartz-grain surfaces (not shown). The predominance of angular grains (up to 90% from 25 grains analyzed for each sample) and their low roundness (~34% from 25 grains analyzed for each sample) indicates that grains have not been altered intensively either by water or by air transportation (Alekseeva, 2005).

Lower hematitic horizons

The important diagnostic feature of paleosol profiles is the presence of a lower red-stained layer (Figure 3a) which is rich in hematite, as indicated by XRD analysis (Figure 5b). These layers of variable thickness occur at different depths from the tops of the paleosols. The thickest (up to 90 cm) red layer is developed at the bottom of P-I. In PS3 the hematitic impregnation is discontinuous, and <10 cm thick.

XRF geochemistry

The distribution of the TiO$_2$/Al$_2$O$_3$ ratio within the pedocomplex indicates periodic inputs of Ti-bearing minerals from the ilmenite-rich substrate material. This sedimentary source of Ti generally increased toward the top of P-I (Figures 4, 5a). This trend may be due to the increase in volcanic activity and/or to textural differences. Paleosols are characterized by large concentrations of
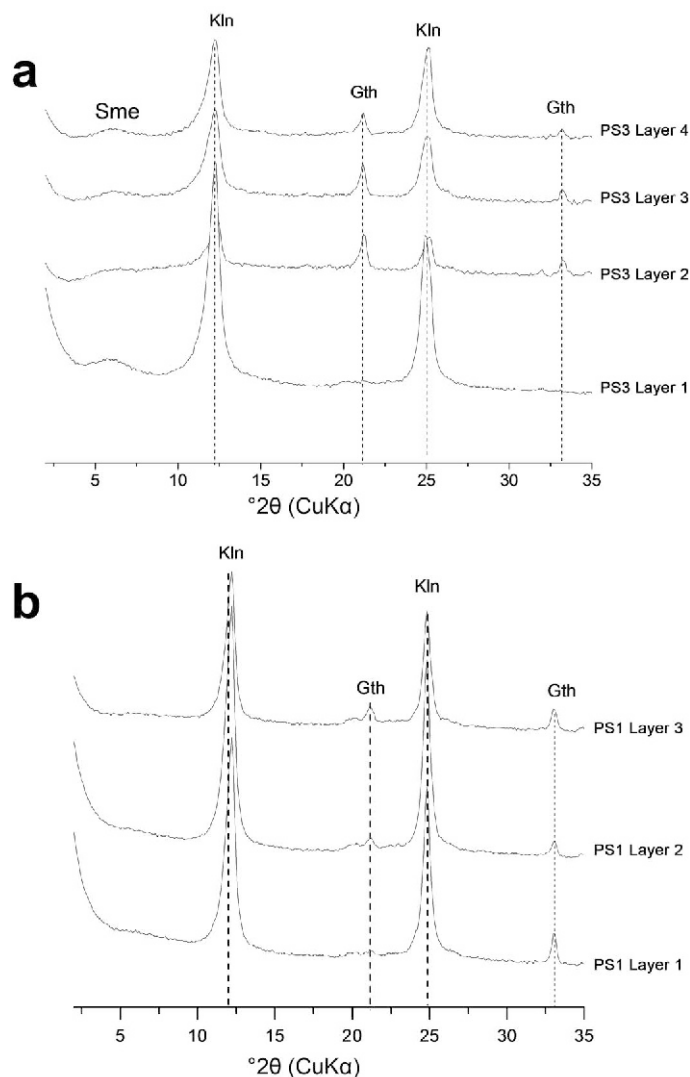
Figure 6. Pedocomplex I. XRD patterns of the clay fraction of Mg-saturated, air-dry samples of paleosol 3 (a) and paleosol 1 (b). Kln − kaolinite; Gth − goethite; Sme − smectite.

Fe_2O_3 which reach 30% in some layers and enlarged values of ratios of $(Fe_2O_3+MnO)/Al_2O_3$ and MnO/Al_2O_3 (Figure 4).

Pedocomplex II

Description. The levee pedocomplex II (P-II) is located between the shale below and Cretaceous deposits above (Figure 2). Pedocomplex II consists of four morphologically and analytically distinct paleosols (PS1−PS4) with a total thickness of ~3 m. PS1 was developed from shale; the other three from volcanigenic material (Figure 7a). At least three inputs of volcanigenic material of intermediate composition took place; these are marked by the enhanced values of TiO_2/Al_2O_3 (Figure 8). The best preserved units of P-II are PS1 and PS3 which are 100 and 80 cm thick, respectively (Figure 7b,c). PS2 and PS4 have been eroded and reworked

intensively and PS4 has been oxidized extensively (Figure 7d). Paleosols 1 and 3 show the clay-rich nature of the upper 50 cm where the clay concentration reaches almost 40% (Figure 8). Volcanic fragments at the bases of paleosols 2 and 3 as well as pedogenic nodules are covered by argilan cutans supporting the suggestion of clay translocation. All paleosols are carbonaceous with siderite contents varying between 2.5 and 8.0% (Figure 8). The Devonian deposits at the top of P-II are the 'reworked'/recycled volcanigenic-sedimentary tuffs-gravels of a sandy texture (6−10% of clay), rich in TiO_2 (11.70−13.28%) and Fe_2O_3 (26.63−48.73%), oxidized extensively, and are characterized by large magnetic susceptibility values (Figure 8). The high concentrations of TiO_2 and Fe_2O_3, and depletion in 'biofriendly' elements, which are characteristic elements for modern soils, such as CaO (0.38−2.77%) and K_2O
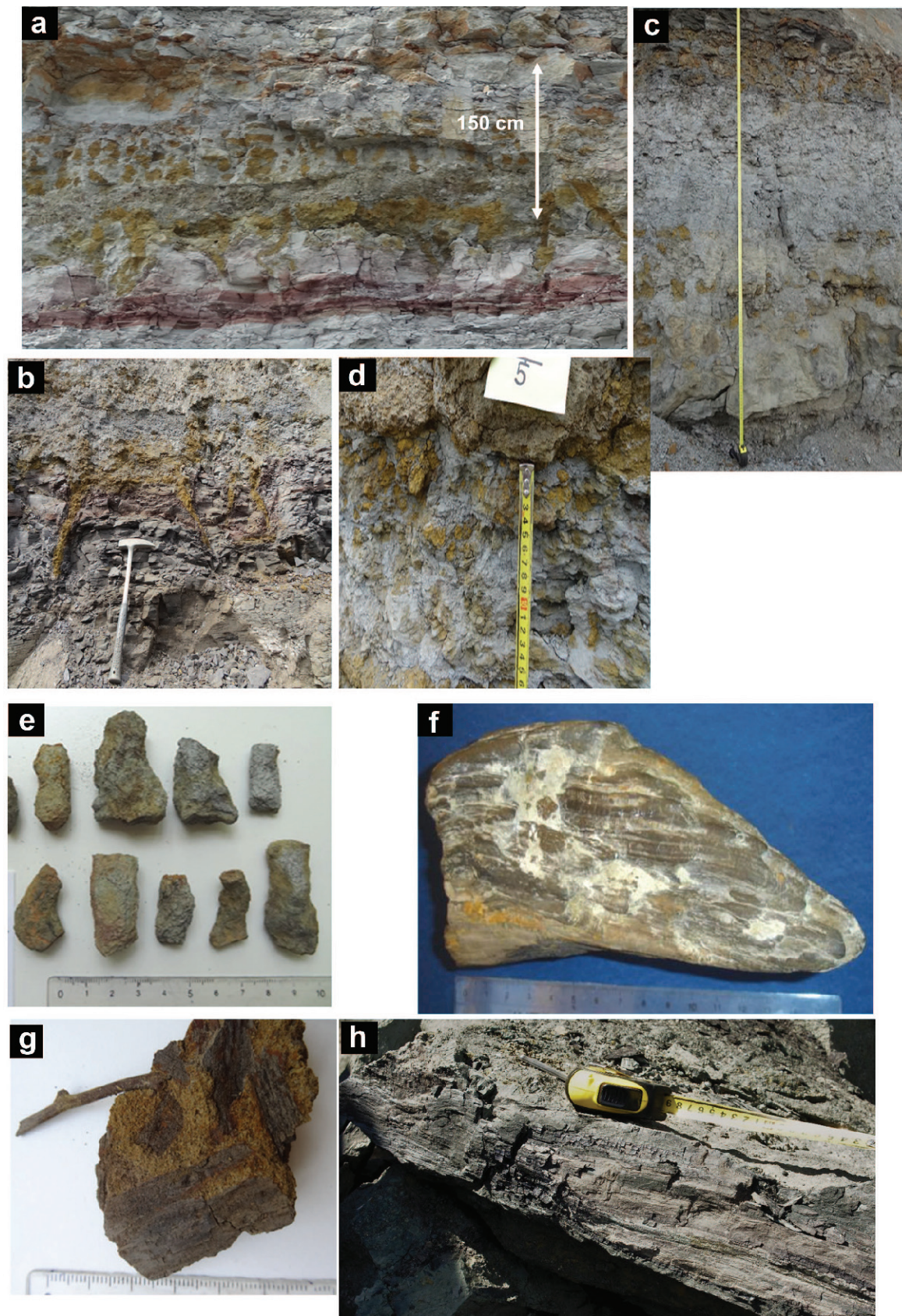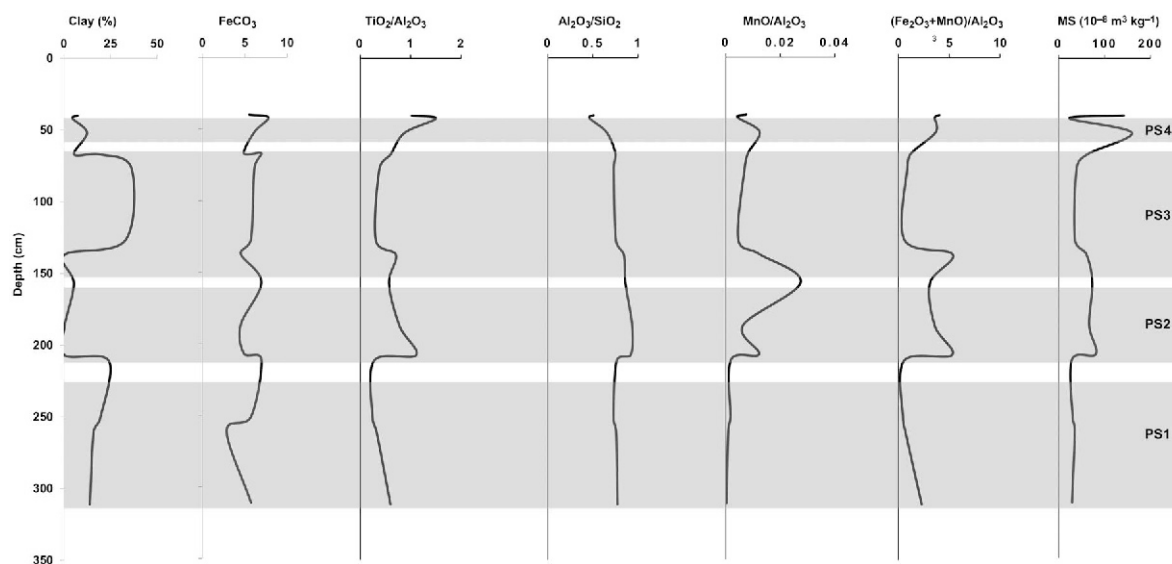
Figure 8. Selected analytical data from pedocomplex II.

(0.04−0.1%), are the principal properties of the Devonian paleosols studied here.

In spite of this geochemical anomaly, Devonian landscapes are characterized by an extreme biodiversity. All subdivisions of P-II have specific imprints of vegetation, most of which are differently preserved roots/rooting systems or roots-derived pedofeatures substituted by siderite and/or goethite (Figures 7b,d,e). Top tuff-gravel layers contain frequent inclusions of ferruginized roots of different size and shape, and wood fragments of *Callyxilon − Archaeopteris* (Figure 7f−h).

Clay mineralogy

The clay mineralogy of paleosols 1−3 is dominated by kaolinite and goethite (Figure 9). Paleosol 4 is montmorillonitic with a smaller amount of kaolinite. The upper part of a shale at the base of P-II is the red-stained hematite layer similar to that at the base of P-I and is probably part of the latter. Development of a single hematite layer at the bank's top, unlike three layers on the channel slope (P-I), reflects the different positions of the water table.

Pedocomplex III

Description. The topographically lowest pedocomplex at the swampy bottom (Figure 2) is composed of at least four hydromorphic organic-rich paleosols (histosols) of ~180 cm total thickness (Figure 10). Paleosols are developed from the laminar, probably alluvial sediments rich in fine sand. All of them are gray partly due to the

abundant inclusions of fine coal particles (Figure 10a,b). The uppermost 10 cm of each paleosol contains fine coalified and pyritized organic detritus, often arranged into large-scale pedofeatures (see below).

Pedocomplex III (P-III) is overlapped by a 30 cm sand layer and then by a 3.5 m tuff of the Yastrebovka Formation with inclusions of volcanic bombs and abundant plant debris, including stem fragments and stumps. Some of the plant debris is coalified and pyritized; other debris retains elements of the original plant structure. Their irregular positions suggest minimal transportation and quick burial. The presence of charcoal specimens can be explained by fires accompanying volcanic explosions. The best preserved paleosol in P-III is the lowest, PS1, ~110 cm thick. In addition to an organic-rich A-horizon, a 10−25 cm thick greenish-yellowish gray, mottled B_0 horizon is developed at 40 cm depth where the Fe_2O_3 concentrations reached 44−48%, *i.e.* ~2 times larger than the mean value for this pedocomplex. As seen from the XRD spectra, the mottles consist entirely of goethite. Material of the lower layer of PS1, assigned to its B_2 horizon, has a blocky, angular structure with ferruginized ped surfaces. In addition, this paleosol has enhanced MnO/Al_2O_3 ratios (Figure 11).

Chemical analysis of paleosols along with large MS values ($48−268 \times 10^{-8}$ m^3 kg^{-1}) has indicated that all parts of the complex are rich in TiO_2 and ferruginized in various ways (Figure 11). Pyrite develops rounded concretions 1−2 cm in diameter. The organic detritus

Figure 7 (*facing page*). Pedocomplex II. (a) Overview showing a hematite layer and wedges at the bottom; (b) wedges from paleosol 1; (c) well preserved profile of paleosol 3 with weathered fragments of lava at the bottom; (d) eroded surface of paleosol 2 with abundant carbonate pedofeatures and overlying lava; (e) roots from paleosol 3; (f−h) wood fragments from the top of the pedocomplex.
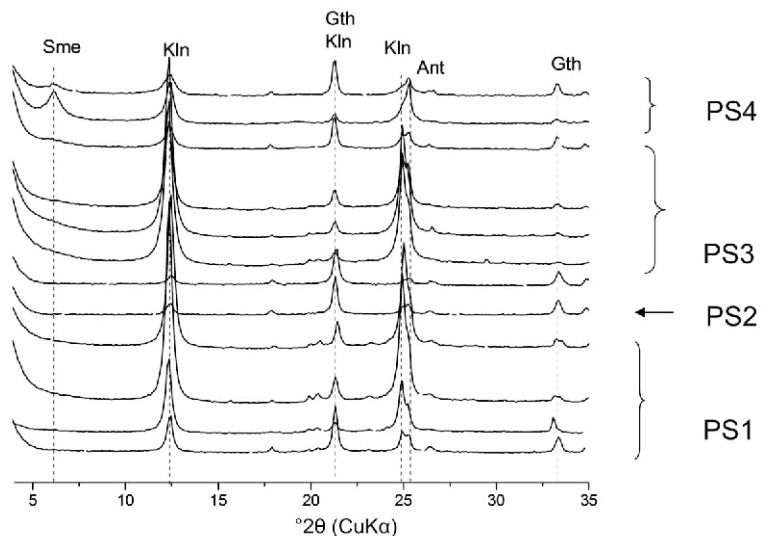
Figure 9. Pedocomplex II. XRD patterns of the clay fractions of Mg-saturated, air-dry samples. Kln − kaolinite, Gth − goethite, Sme − smectite, Ant − anatase.

contains inclusions of *Oresvovia voronejiensis* phytoleims (Figure 10b). The latter are golden-brown in color and well preserved. *Orestovia* is a transitional form between the algae-like *Protosalvinia* and a sporangiate vascular plant with a thick cuticle. This plant was first discovered within Devonian deposits in Pavlovsk (Istchenko and Istchenko, 1981). Coalified organic detritus together with *Orestovia* phytoleims creates
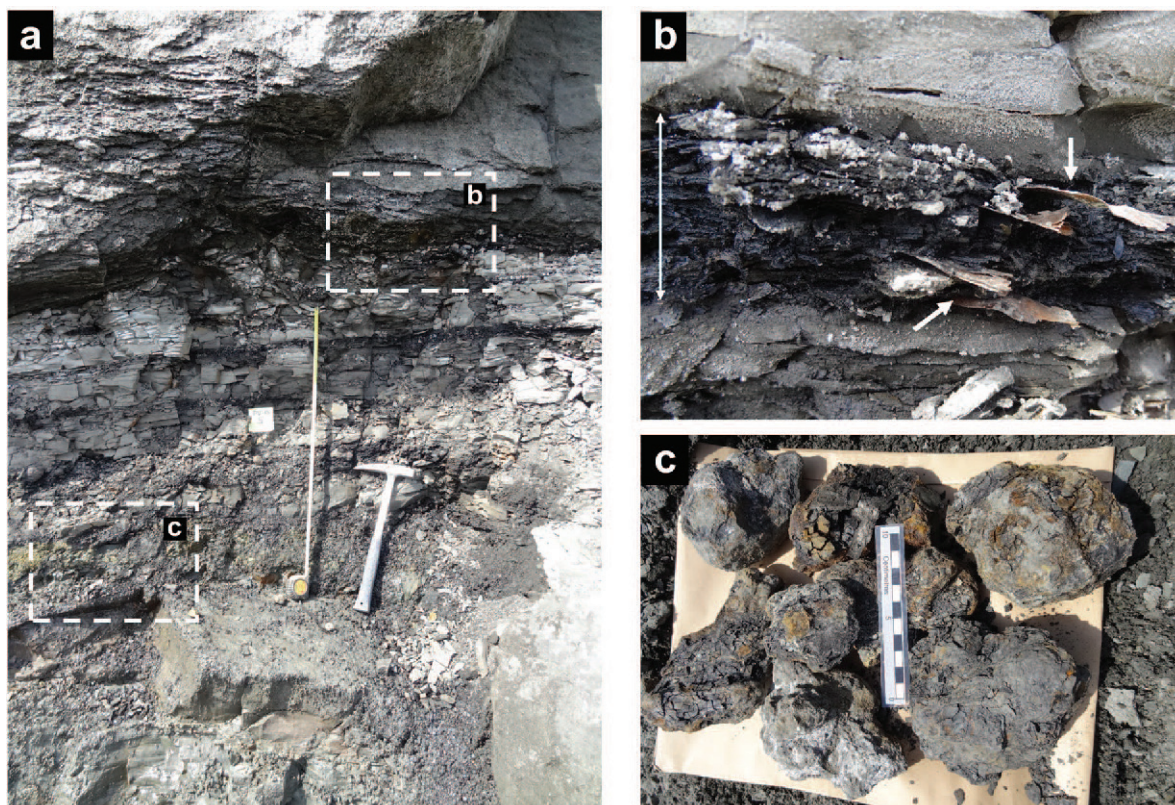

Figure 10. Pedocomplex III. (a) Overview; (b) *Orestovia* within the coalified layer at the top of paleosol 4 (arrows). Scale = 10 cm; (c) coal-pyrite concretions from the top of paleosol 1.
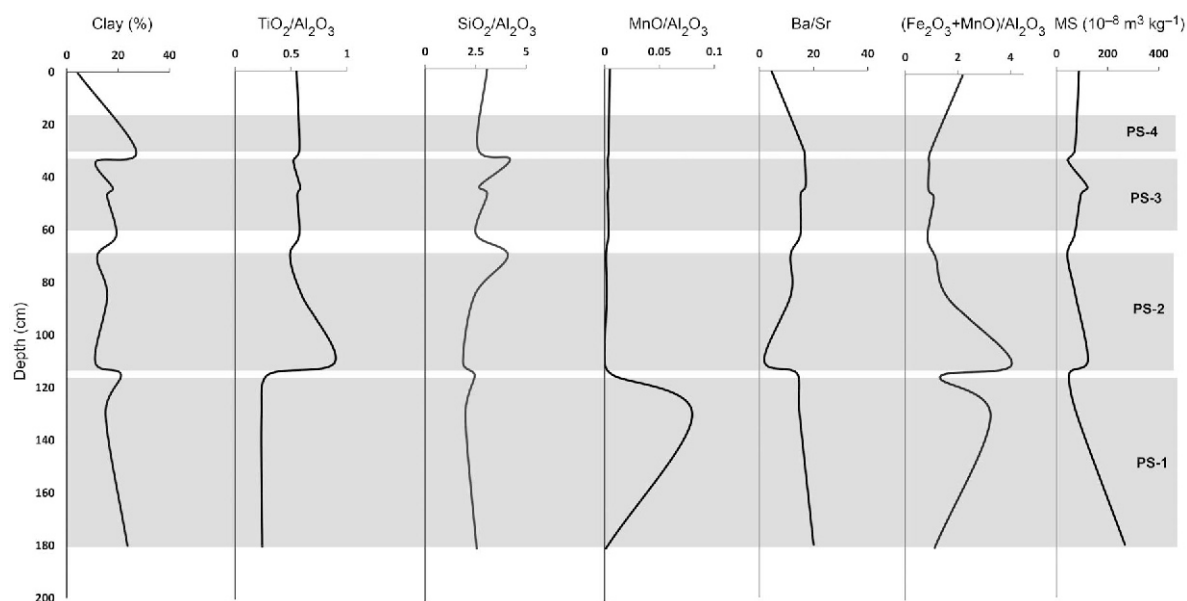
Figure 11. Selected analytical data of pedocomplex III.

large (up to 15 cm) pedo-features, concretions of flat and irregular shape, cemented with fine pyrite (Figure 10c). The features are arranged into discrete individual layers (horizons) which clearly mark the tops of each P-III paleosol.

Clay mineralogy

The clay fractions of all paleosols contain kaolinite and dioctahedral smectite in more or less equal proportions. The smectite is a low-charged montmorillonite of Wyoming type, morphologically similar to that described by Chipera and Bish (2001). Traces of mica occur in PS1 only (Figure 12).

The grayish-blue hues, abundant pyrite of different generations, and plant coalification suggest that this pedocomplex was developed under concurrent and/or early diagenetic anoxic environments, as also indicated by the decrease in MS values toward the top of each profile (Figure 11). On the other hand, the enhanced values of Ba/Sr ratio suggest a freshwater sedimentary environment (Makhlina *et al*., 1993).

Vegetation imprint

The terrestrial middle−late Devonian deposits contain huge varieties of fossil plants including some unique species such as: *Orestovia voronejiensis, Tanaitis furcihasta*, and *Istchenkophyton filiciforme* (Istchenko and Istchenko, 1981; Krassilov *et al*., 1987; Broushkin and Gordenko, 2009). Field observations revealed well preserved fragments of arborescent plants including branches, stems, and stumps, numerous small forms, and numerous imprints (Figures 7f−h, 10c). Forest vegetation represented mainly by progymnospermous plants was polyspecific with predominantly large arche-

opterid trees (Figure 7f,h). Other terrestrial vegetation such as woody progymnospermous shrubs (*Tanaitis* and *Svalbardia*), cladoxylalean ferns (*Pseudosporochnales*), different licopsids, and small-sized plants (such as rhyniophytes) were also distributed widely.

Earth's Devonian history is referred to as the 'Devonian explosion' with the greening of land by vascular plants, the appearance of arborescent plants and the first forests, the extreme biodiversity with a broad distribution of lycopsids, propteridophyta, progymnospermous, and the first calamites. At the same time different transitional forms between the algae-like *Protosalvinia* and the sporangiate vascular plants existed that are preserved locally in deposits as phytoleims. In the Devonian deposits of Pavlovsk, two types of these plans were discovered and described in detail (Istchenko and Istchenko, 1981): *Orestovia* and *Bitelaria*, belonging
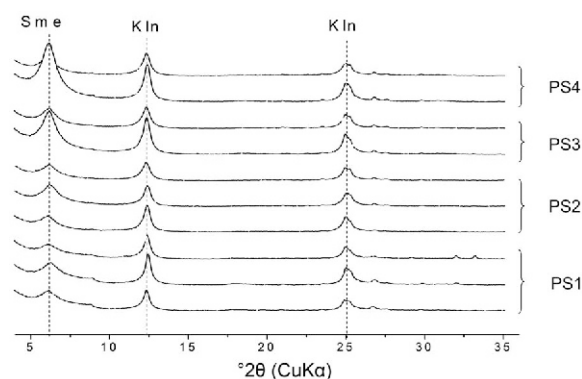

Figure 12. Pedocomplex III. XRD patterns of the clay fractions of Mg-saturated, air-dry samples. Kln − kaolinite, Sme − smectite.

to red and brown algae. Later, these species were attributed to remnants of *Schuguria ornata* at Tschirkova-Zalesskaya (Broushkin and Gordenko, 2016). In the deposits studied here, such remnants have developed large accumulations without admixture of other species, probably creating the dense monocultures occupying the shallow-water basins and coastal environments. The thick cuticle of these remnants indicates that the locations they occupied dried periodically which might be related to increasing aridity. The broad distribution of these plants in the Devonian deposits studied may indicate the seasonality of climate with distinct wet-and-dry seasons. Recently, a new, thick-cuticled plant was discovered (*Istchenkophyton filiciforme* gen. et sp. nov) in Devonian deposits of the Pavlovsk quarry (Broushkin and Gordenko, 2009). Those authors explained its unique anatomy as being due to the adaptation to unfavorable conditions, *i.e.* temporary (seasonal?) water deficit, such as relatively raised spots in a floodplain, banks of ephemeral streams, *etc*.

Root systems

To date, few findings have been made of *in situ*, well preserved roots or other below-ground plant structures of Paleozoic age (*e.g.* Driese and Mora, 1993; Algeo and Scheckler, 1998; Cox *et al.*, 2001; Raven and Edwards, 2001; Stein *et al*., 2007, 2012; Morris *et al.*, 2015; Retallack, 2015; Tabor and Myers, 2015). Well preserved Paleozoic rooting systems were found (Morris *et al.*, 2015) along with other *in situ* vegetation in parts of North American territory. Two types of fine (up to 6 mm in diameter), coalified roots with non-preserved tissues in late Devonian paleosols of Timan (Russia) were found by Shumilov (2010, 2013).

The paleosols studied from P-I and P-II contain abundant individual roots and root systems of different morphology and size. The diameter of individual roots varies between several mm and >10 cm and the length between 1 and 60 cm with a median of 15 cm. The roots were preserved in various states, depending on their location. The PS3 profile from P-I, which was overlain catastrophically by estuarial argillite, is uniquely preserved, including the litter layer. The rooting systems of rapidly buried living plants preserved the pipe-like shape and often some tissues: parenchyma, secondary crust, and inner and external exoderm (Figure 3b,c). These root systems are suggested here to belong to primitive progymnosperms similar to *Tanaites*. Numerous spores of such plants were found in the litter layer of PS3 (Figure 3g). The tissues of the rhizocreations studied were substituted with siderite and (hydro)goethite, probably being a diagenetic product of siderite oxidation.

Because of the warm Devonian subtropical climate, high temperatures, low atmospheric O_2 concentration, and high concentrations of Fe_2O_3 in host rocks, much soluble Fe^{2+} was available and taken by roots. High concentrations of CO_2/HCO_3 in soil solutions and deficits in terms of Ca^{2+} favored the precipitation of siderite (Tabor and Myers, 2015).

On the other hand, the root systems of a partly eroded profile of PS1 from P-II have been degraded completely and are present as wedges up to 30 cm long and up to 15 cm wide (Figure 7b). Up to six such wedges occur per meter. The inner parts of the wedges consist of a loose soft yellow material, containing about twice as much clay as the host rock (37 and 20% clay, respectively) and 68% of Fe_2O_3 as the siderite/goethite mixture. Their outer red edges contain hematite. Frequent fragments of *Callixylon* may indicate that these large-scale rooting systems probably belong to *Archaeopteris.* The upland location of P-II suggests that these plants were common not only in wet floodplain habitats but also created the upland forests.

The rooted plants played a crucial biochemical role in formation of the Devonian CZ by crushing rocks, increasing the rate of weathering and pedogenesis, mobilization of plant nutrients, and enhancing the geochemical cycles of elements, thus increasing the flux of elements into the ocean and mitigating the atmospheric CO_2 (Mora *et al.*, 1996; Cox *et al.*, 2001; Berner, 2004; Mintz *et al.*, 2010). In addition, the development of rooting systems provided the substrate disintegration, influenced water and air exchange, and reduced surface runoff and erosion rates.

Paleoclimate reconstruction

Except for quantifying the paleoweathering intensity, the geochemical weathering indices may serve to estimate the paleoclimate parameters, *i.e.* the mean annual precipitation (MAP) and the mean annual temperature (MAT) *via* empirical transfer functions (Sheldon and Tabor, 2009). The MAP values were calculated here using XRF results and equations (standard error of ±180 mm), following the method of Sheldon *et al*. (2002):

MAP1= −259.3ln (ΣBases/Al)+759,
where (ΣBases/Al = (Ca+Mg+Na+K)/Al)

MAP2 = 221.1$e^{0.0179(CIA-K)}$,
where ((CIA-K) = [Al/(Al+Na+Mg+Ca)] × 100).

The MAP values obtained range between 900 and 1200 mm (±180 mm) which, along with the presence of the kaolinite-goethite-hematite mineral associations of the paleosols and host rocks, testify to the wet-warm, tropical type of middle−late Devonian climate in the given equatorial territory (Figure 13). The distribution of *Oresvovia voronejiensis, Schuguria ornate*, and *Istchenkophyton filiciforme* all having thick cuticles suggests the seasonal aridity of the climate. North American occurrences at ~40ºS paleolatitude also suggest a warm climate with distinct wet-and-dry seasons during the late Devonian period (Driese and Mora, 1993; Cox *et al*., 2001; Cressler, 2006).
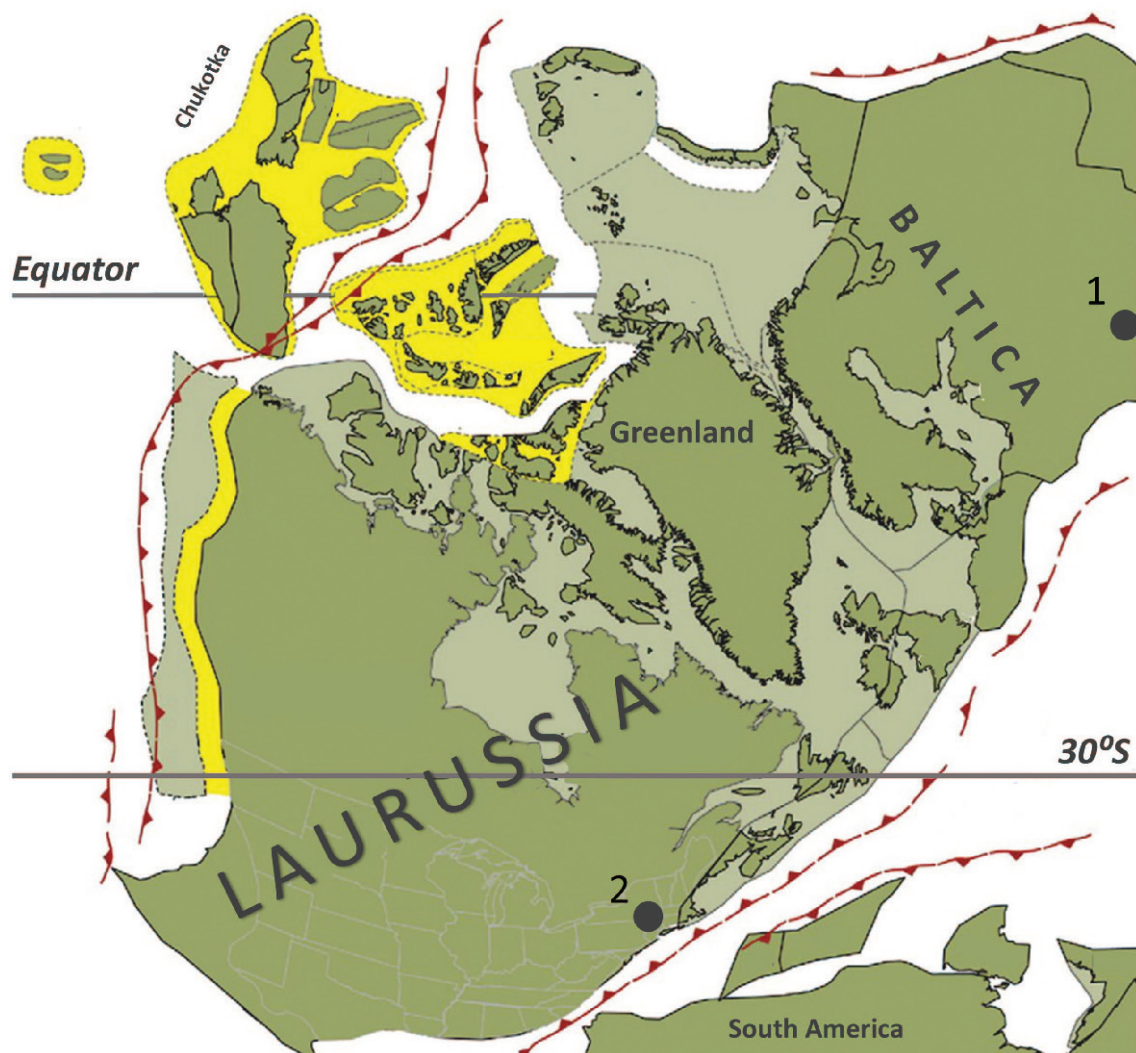
Figure 13. Terrane map of western and central Laurussia (including the Laurentian sector) and adjacent areas in the late Devonian (Famennian) from Cocks and Torsvik (2011) with locations of Pavlovsk (1) and New York (2).

DISCUSSION

During the middle−late Devonian period the territory studied had a pronounced relief with automorphic (watershed), semi-hydromorphous (slope), and at least seasonally waterlogged (wetland) conditions of pedogenesis. These landscapes and corresponding paleosols differ from the dominant middle−late Devonian pedosphere described as marine-influenced, coastal−fluvial wetlands, waterlogged and poorly oxygenated (Griffing et al., 2000; Cressler, 2006; Stein et al., 2012). Some paleosols from this unique site were oxidized intensely. Semi-hydromorphous and seasonally waterlogged paleosols from the slope and channel bottom had probably also undergone stages when oxidizing conditions prevailed. Enhancements of $(Fe_2O_3+MnO)/Al_2O_3$ values in paleosol profiles (Figures 4, 8, 11), which reflect the degree of material oxidation, show enhancements for

pedogenically reworked materials (Kalinin and Alekseev, 2011).

The pronounced relief caused the differentiation of water regimes but in both cases the drainage conditions were favorable, partly due to the sandy texture and inclusions of volcaniclastic and tuffaceous porous rocks. As a consequence, the soil cover consisted of different soil types and was not restricted to vertic, non-differentiated, smectitic lithogenic soils as was found in other studies (Driese and Mora, 1993; Cressler, 2006; Brasier et al., 2014). Paleosols from P-I and P-II had well pronounced texturally and chemically differentiated profiles with production and translocation of kaolinitic clay, pedogenic carbonate nodules, organic matter, and in situ roots. The prevalence of kaolinite in a felsic parent rock reflects the favorable conditions for chemical weathering (warm/humid climate, good drainage)

and long duration of exposure. The only bed which can be regarded as having been water saturated permanently is the argillite layer at the top of PS3 from P-I (Figure 2). The other catastrophic factor, volcanic activity, permitted denudation of the soil cover and supplied a parent material for the subsequent pedogenesis. As a consequence, all the paleosols studied were stacked and arranged into pedocomplexes of up to four individual paleosol profiles. Two types of profiles proposed by Mariott and Wright (1993) can be applied to describe the environments studied here: (1) a composite one developed under rapid, intermittent, and medium sedimentary accumulation; and (2) a compound type developed under rapid, intermittent, and large sedimentary accumulation. In the case of type 1, partly eroded overlapped profiles with overprinting were detected; in the case of type 2, a complete, well preserved profile without overprinting was observed. Most of the paleosols studied having partly eroded overlapped profiles with overprinting belong to type 1 and only one, PS3 from P-I, having a complete, well preserved profile without overprinting, belongs to type 2. The main type of deposit in the Yastrebovka Formation is of volcanigenic-sedimentary origin. Lava supplied the system with Fe which is the most distinct typomorphic element in this paleo-CZ. A wet and warm climate along with dense vegetation accelerated the Fe mobilization which replaced Ca in pedogenic carbonate nodules, rhizocretions, stromatolites, and marine carbonates. Based on the iron mineralogy, the multistage development of the landscape can be described as follows: (1) formation of well drained, aerated profiles having red hematitic layers at the base; (2) periodic flooding with intermittent sedimentary accumulation, frequently containing plant debris, provided anoxic conditions and siderite/pyrite substitution of roots and other plant fragments from the overlapped soils occurred as a result; and (3) surface exposure causing partial or complete transformation of siderite to goethite and subsequent formation of a new red hematitic layer. The sedimentary accumulation events changed, among other things, the vegetation communities.

CONCLUSIONS

The unique paleogeographic conditions and tropical climate during the middle−late Devonian in what is now southeastern Russia created a complex paleo-CZ consisting of several paleo sub-CZs representing the chronological sequences in each of three sites studied. In addition, linked to the paleorelief, the sites studied could be considered as a paleo-toposequence. The soils in these sites were developed under various kinds of vegetation and probably differed in terms of time taken to develop. The climate, determined by the equatorial location of the territory, was more or less stable (Figure 13). Over time, single sub-CZs were combined

step-by-step *via* atmospheric water circulation, rooting systems, and elemental cycles which overprinted the previous stages of pedogenesis.

The site studied in Russia differs fundamentally from the well described Givetian−Frasnian forest at Gilboa (New York, USA) discovered in the 1870s and studied extensively since the 1920s (Stein *et al.*, 2007, 2012). The Gilboa complex forest community belonged to a tropical muddy swamp near the palaeo-shoreline. The paleosols of Pavlovsk (at least some of them) are automorphic, deeply weathered, extensively oxidized, ferruginized, and deeply reworked by rooting systems of diverse plants, including arborescent vegetation. In the waterlogged part of the paleo-relief, hydromorphous paleosols under *Orestovia / Schuguria* were developed.

In spite of significant differences between environments and most components of modern and Devonian CZs, their key components, rooted (tropical in the present case) soils, demonstrate a number of similarities and were developed at least partly under similar processes. Both environments demonstrate the deep chemical weathering of sediments, typomorphism of iron, clay production and redistribubution, and kaolinite/ goethite mineral assemblage, amongst other features.

Paleo-CZ studies are very worthwhile. Paleosols are unique and the most reliable natural archive of Earth's terrestrial life. The virgin states of the parent sediments and single authigenesis of Devonian soils, compared with the multiply recycled material of most modern soils, allow them to be used as simple natural systems for the modeling of soil processes in modern CZs. On the other hand, similar modern soils and CZs provide an invaluable source of data which allows the reconstruction of the early Earth's environments.

REFERENCES

Alekseev, A.O., Kabanov, P.B., Alekseeva, T.V., and Kalinin, P.I. (2015) Magnetic susceptibility and geochemical characterization of a Late Mississippian cyclothemic section Polotnyanyi Zavod, (Moscow Basin, Russia). Pp. 181−196 in: *Magnetic Susceptibility Application: A Window onto Ancient Environments and Climatic Variations* (A.C. Da Silva, M.T. Whalen, J. Hladil, L. Chadimova, D. Chen, S. Spassov, F. Boulvain and X. Devleeschouwer, editors). Special Publications, **414**, Geological Society, London.
Alekseeva, V.A. (2005) Micromorphology of quartz grain surface as indicator of glacial sedimentation conditions: evidence from the Protva river basin. *Lithology and Mineral Resources*, **40**, 420−428.

Algeo, T.A. and Scheckler, S. E. (1998) Terrestrial-marine teleconnections in the Devonian: links between the evolution of land plants, weathering processes, and marine anoxic events. *Royal Society of London Philosophical Transactions (B): Biological Sciences*, **353**, 113−130.

Amundson, R., Richter, D.D., Humphreys, G.S., Jobbagy, E.G., and Gaillardet, J. (2007) Coupling between biota and earth materials in the Critical Zone. *Elements*, **3**, 327−332.

Berner, R.A. (2004) *The Phanerozoic Carbon Cycle: CO$_2$ and O$_2$*. Oxford University Press, Oxford, New York.

Brasier, A.T., Morris, J.L., and Hillier, R.D. (2014) Carbon isotopic evidence for organic matter oxidation in soils of the Old Red Sandstone (Silurian to Devonian, South Wales, UK). *Journal of the Geological Society (London)*, **171**, 621−634.

Broushkin, A.V. and Gordenko, N.V. (2009) *Istchenkophyton filiciforme* gen. et sp. nov., a new small vascular plant with thick cuticle from the Devonian of Voronezh Region (European Russia). *Paleontological Journal*, **43**, 1202−1216.

Broushkin, A.V. and Gordenko, N.V. (2016) Devonian flora of Middle−Lower Povolz'e. *Phytodiversity of Eastern Europe*, **1**, 14−32 (in Russian).

Chipera, S.J. and Bish, D.L. (2001) Baselines studies of the Clay Minerals Society source clays: powder X-ray diffraction analyses. *Clays and Clay Minerals*, **49**, 398−409.

Chorover, J., Kretzschmar, R., Garcia-Pichel, F., and Sparks, D.L. (2007) Soil biogeochemical processes within the Critical Zone. *Elements*, **3**, 321−326.

Cocks, L.R.M. and Torsvik, T.H. (2011) The Palaeozoic geography of Laurentia and western Laurussia: A stable craton with mobile margins. *Earth-Science Reviews*, **106**, 1−51.

Cox, J.E., Railsback, L.B., and Gordon, E.A. (2001) Evidence from Catskill pedogenic carbonates for a rapid Late Devonian decrease in atmospheric carbon dioxide concentrations. *Northeastern Geology and Environmental Sciences*, **23**, 91−102.

Cressler, W.L. (2006) Plant paleoecology of the Late Devonian Red Hill locality, north-central Pennsylvania, an Archaeopteris-dominated wetland plant community and early tetrapod site. *Geological Society of America Special Papers*, 79−102.

Davies, N.S. and Gibling, M.R. (2010) Paleozoic vegetation and the Siluro-Devonian rise of fluvial lateral accretion sets. *Geology*, **38**, 51−54.

Driese, S.G. and Mora, C.I. (1993) Physico-chemical environment of pedogenic carbonate formation in Devonian vertic paleosols, Central Appalachians, USA. *Sedimentology*, **40**, 199−216.

Giardino, J.R. and Houser, Ch. (2015) *Principles and Dynamics of the Critical Zone*, 1st edition. Elsevier, Amsterdam.

Griffing, D.H., Bridge, J.S., and Hotton, C.L. (2000) Coastal-fluvial palaeoenvironments and plant palaeoecology of the Lower Devonian (Emsian), Gaspe Bay, Quebec, Canada. Pp. 61−84 in: *New Perspectives on the Old Red Sandstone* (P.F. Friend and P.B.J. Williams, editors). Geological Society, London, UK.

Hillier, R.D., Edwards, D., and Morrissey, L.B. (2008) Sedimentological evidence for rooting structures in the Early Devonian Anglo-Welsh Basin (UK), with speculation on their producers. *Palaeogeography, Palaeoclimatology, Palaeoecology*, **270**, 366−380.

Istchenko, T.A. and Istchenko, A.A. (1981) *Middle Devonian Flora of the Voronezh Anteclise*. Naukova Dumka, Kiev (in Russian).

Kabanov, P.B., Alekseeva, T.V., Alekseeva, V.A., Alekseev, A.O., and Gubin, S.V. (2010) Paleosols in Late Moscovian

(Carboniferous) marine carbonates of the East European Craton revealing "Great calcimagnesian plain" landscapes. *Journal of Sedimentary Research*, **80**, 195−215.

Kabanov, P.B., Alekseev, A.O., and Zaitsev, T. (2014) The Late Viséan−Serpukhovian in the type area for the Serpukhovian Stage (Moscow Basin, Russia): Part 2. Bulk geochemistry and magnetic susceptibility. *Geological Journal*, **51**, 195−211.

Kalinin, P.I. and Alekseev, A.O. (2011) Geochemical characterization of loess-soil complexes on the Terek-Kuma Plain and the Azov-Kuban' Lowland. *Eurasian Soil Science*, **44**, 1315−1332.

Kornilovich, B.Yu. (1994) *Structure and Surface Chemistry of Mechano-Chemical treated Layer Silicates and Carbonates.* Naukova Dumka, Kiev, Russia (in Russian).

Krassilov, V.A., Raskatova, M.G., and Istchenko, A.A. (1987) A new archaeopteridaliean plant from the Devonian of Pavlovsk, U.S.S.R. *Review of Palaeobotany and Palynology*, **53**, 163−173.

Lebedev, O.A., Luksevics, E., and Zakharenko, G.V. (2010) Palaeozoogeographical connections of the Devonian vertebrate communities of the Baltica Province. *Palaeoworld*, **19**, 108−128.

Levikh, N.N. (1988) *Geneticheskie osobennosti kaolinitov Belorussii*. Nauka i technika, Minsk, Russia (in Russian).

Lin, H. (2010) Earth's Critical Zone and hydropedology: concepts, characteristics, and advances. *Hydrology and Earth System Sciences*, **14**, 25−45.

Makhlina, M.Kh., Vdovenko, M.V., Alekseev, A.S., Byvsheva, T.V., Donakova, L.M., Zhulitova, V.E., Kononova, L.I., Umnova, N.I., and Shik, E.M. (1993) *Nizhniy carbon Moskovskoy sineklizy i Voronezhskoy anteklizy*. Nauka, Moscow (in Russian).

Marriott, S.B. and Wright, V.P. (1993) Palaeosols as indicators of geomorphic stability in two Old Red Sandstone alluvial suites, South Wales. *Journal of the Geological Society (London)*, **150**, 1109−1120.

Mintz, J.S., Driese, S.G., and White, J.D. (2010) Environmental and ecological variability of Middle Devonian (Givetian) forests in Appalachian basin paleosols, New York, United States. *Palaios*, **1**, 85−96.

Mora, C.I., Driese, S.G., and Colarusso, L.A. (1996) Middle to Late Paleozoic atmospheric CO$_2$ levels from soil carbonate and organic matter. *Science*, **271**, 1105−1107.

Morris, J.L., Leake, J.R., Stein, W.E., Berry, Ch.M., Marshall, J.E.A., Wellman, C.H., Milton, J.A., Hillier, S., Mannolini, F., Quirk, J., and Beerling, D.J. (2015) Investigating Devonian trees as geo-engineers of past climates: linking paleosols to palaeobotany and experimental geobiology. *Paleontology*, **58**, 787−801.

Nikishin, A.M., Ziegler, P.A., Stephenson, R.A., Cloetingh, S.A.P.L., Furne, A.V., Fokin, P.A., Ershov, A.V., Bolotov, S.N., Korotaev, M.V., Alekseev, A.S., Gorbachev, V.I., Shipilov, E.V., Lankreijer, A., Bembinova, E.Yu., and Shalimov, I.V. (1996) Late Precambrian to Triassic history of the East European Craton: dynamics of sedimentary basin evolution. *Tectonophysics*, **268**, 23−63.

Nordt, L.C. and Driese, S.D. (2014) Application of the critical zone concept to the deep-time sedimentary record. *The Sedimentary Record*, **11**, 4−9.

Nordt, L.C., Hallmark, C.T., Driese, S.G., Dworkin, S.I., and Atchley, S.C. (2012) Biogeochemical characterization of a lithified paleosol: Implications for the interpretation of ancient Critical Zones. *Geochimica et Cosmochimica Acta*, **87**, 267−282.

Quast, A., Hoefs, J., and Paul, J. (2006) Pedogenic carbonates as a proxy for palaeo-CO$_2$ in the Palaeozoic atmosphere. *Palaeogeography, Palaeoclimatology, Palaeoecology*, **242**, 110−125.

Raskatova, M.G. (1990) *Palinokompleksi pogranichnih Givetian-Frasnian otlozenii Centralnogo Devoskogo polya i Timana*. PhD thesis, Moscow State University, Moscow, Russia (in Russian).

Raskatova, M.G. (2004) Miosporovaya zonalnost sredne-verhnedevonskih otlozeniy ugo-vostochnoi chasti Voronezskoi anteclizi (Pavlovskii kar'er). *Vestnik Voronezskogo Universiteta. Geologia*, **2**, 289−298 (in Russian).

Raven, J.A. and Edwards, D. (2001) Roots: evolutionary origins and biogeochemical significance. *Journal of Experimental Botany*, *Roots special Issue*, **52**, 381−410.

Retallack, G.J. (2001) *Soils of the Past: an Introduction to Paleopedology*. 2nd edition. Malden, USA, Blackwell Science, Oxford, UK.

Retallack, G.J. (2015) Silurian vegetation stature and density inferred from fossil soils and plants in Pennsylvania, USA. *Journal of the Geological Society (London)*, **121**, 621−634.

Rodionova, G.D., Umnova, V.T., Kononova, L.I., Ovnatanova, N.S., Rzonsnizkaya, M.A., and Fedorova, T.I. (1995) *Devon Voronezskoi anteclizi i Moscovskoi sineclizi*. Central Regional Geological Survey, Moscow (in Russian).

Sheldon, N.D. and Tabor, N.J. (2009) Quantitative paleoenvironmental and paleoclimatic reconstruction using paleosols. *Earth Sciences Review*, **95**, 1−52.

Sheldon, N.D., Retallack, G.J., and Tanaka, S. (2002) Geochemical climofunctions from North American soils and application to Paleosols across the Eocene−Oligocene boundary in Oregon. *The Journal of Geology*, **110**, 687−696.

Shevyrev, L.T., Savko, A.D., and Shishov, A.V. (2004) Evoluziya tektonicheskoi structure Voronezhskoi anteklizi i ee endogennii rudogenez. *Trudi Voronezhskogo Universiteta*, **25**, 1−192 (in Russian).

Shumilov, I.Ch. (2010) The first discovery of paleosols in green Devonian sediments of middle Timan. *Doklady Earth Sciences*, **434**, 1303−1305.

Shumilov, I.Ch. (2013) Preservation conditions of *in situ* root systems in Devonian sections of the middle Timan region.

Lithology and Mineral Resources, **48**, 65−73.

Shumilov, I.Ch. and Mingalev, A.N. (2009) First find of paleosols in the Devonian red deposits of the middle Timan. *Doklady Earth Sciences*, **428**, 1080−1082.

Stein, W.E., Mannolini, F., Hernick, L., Landing, E., and Berry, Ch.M. (2007) Giant Cladoxylopsid trees resolve the enigma of the Earth's earliest forest stumps at Gilboa. *Nature*, **446**, 904−907.

Stein, W.E., Berry, Ch.M., Hernick, L., and Mannolini, F. (2012) Surprisingly complex community discovered in the mid-Devonian fossil forest at Gilboa. *Nature*, **483**, 78−81.

Tabor, N.J. and Myers, T.S. (2015) Paleosols as indicators of paleoenvironment and paleoclimate. *Annual Review of Earth and Planetary Sciences*, **43**, 333−361.

van Reeuwijk, L.P. (editor) (2002) *Procedures for Soil Analysis*, (6th edition), ISRIC Technical paper 9, Wageningen, The Netherlands.

Weibel, R., Lindstrom, S., Pedersen, G.K., Johansson, L., Dybkjaer, K., and Whitehouse, M.J. (2016) Groundwater table fluctuations recorded in zonation of microbial siderites from end-Triassic strata. *Sedimentary Geology*, **342**, 47−65.

Wilkinson, M., Haszeldine, R.S., Fallick, A.E., and Osborne, M.J. (2000) Siderite zonation within the Brent Group: microbial influence or aquifer flow? *Clay Minerals*, **35**, 111−121.

Zamanian, K., Pustovoytov, K., and Kuzyakov, Y. (2016) Pedogenic carbonates: Forms and formation processes. *Earth-Science Reviews*, **157**, 1−17.

Zavarzin, G.A. (2008) Microbial biosphere. Pp. 25−44 in: *Biosphere Origin and Evolution* (N. Dobretsov, N. Kolchanov, A. Rozanov, and G. Zavarzin, editors). Springer, Berlin.

Zolotareva, G.S. (2009) Typomorphism i typochimism Ti-Zr rossipei Voronezhskoi anteklizi kak kriterii reconstrukzii usloviy ih formirovaniya. PhD thesis, Voronezh University, Russia (in Russian).